Absorption Spectra and Photophysical Properties of a Series of Polypyridine Ligands Containing Appended Pyrenyl and Anthryl Chromophores and of Their Ruthenium(II) and Osmium(II) Complexes

Béatrice Maubert,[†] Nathan D. McClenaghan,[†] Maria Teresa Indelli,[‡] and Sebastiano Campagna*,[†]

Dipartimento di Chimica Inorganica, Chimica Analitica e Chimica Fisica, Università di Messina, Via Sperone 31, 98166 Messina, Italy, and Dipartimento di Chimica, Università di Ferrara, Via L. Borsari 46, 44100 Ferrara, Italy

Received: June 5, 2002; In Final Form: October 16, 2002

The absorption spectra and luminescence properties (both in fluid solution at room temperature and in rigid matrix at 77 K) of four polypyridine ligands substituted with pyrenyl and anthryl chromophores have been investigated, together with the same properties of 15 Ru(II) and Os(II) complexes prepared using the same ligands. Absorption spectroscopy revealed that the various chromophores contribute to the overall absorption spectra of the mixed-chromophore species in a roughly additive way. The photophysical investigations allowed us to obtain information on several aspects. For example, in the mixed pyrene−anthracene bipyridine-based systems, efficient singlet−singlet pyrene-to-anthracene energy transfer takes place, whereas the same process involving the triplet states is apparently not efficient, unless a metal-to-ligand charge-transfer (MLCT) excited-state mediates the process. The luminescence properties of the Ru(II) complexes are dominated by ^{3}MLCT levels at room temperature (with a few exceptions, that is, the anthracene-containing species) and by pyrene- and/or anthracene-based triplet states at 77 K. However, at room-temperature, equilibration between ^{3}MLCT and pyrene triplets levels is established, and as a consequence, the luminescence lifetimes of the complexes are significantly prolonged (up to 18 μs for the species containing six pyrenyl chromophores). This excited-state lifetime prolongation is linearly related to the number of pyrenyl chromophores and is independent of connectivity. The photophysical properties of the Os(II) complexes are dominated by ^{3}MLCT levels both at room temperature and at 77 K. However, the anthryl chromophores clearly influence the excited-state lifetime of these complexes at room temperature. Indeed, although the anthracene-based triplet states lie at higher energy than the ^{3}MLCT levels, an excited-state equilibration process is also established, as clearly demonstrated by transient absorption spectroscopy, and the luminescence lifetime is (slightly) extended.

Introduction

Ruthenium(II) and osmium(II) polypyridine complexes are playing leading roles in the development of supramolecular (multicomponent) artificial systems for photochemical conversion of solar energy and elaboration of information at the molecular level.[1] In all of the studied systems based on these species, Ru(II) and Os(II) complexes act as the photoactive subunits, because they are capable of collecting visible light and driving photoinduced electron- and/or energy-transfer processes, which form the basis of the properties of the functional supramolecular arrays. A fundamental requisite that makes Ru(II) and Os(II) polypyridine complexes quite useful for many potential applications is their relatively long-lived lowest-lying excited state, formally a triplet metal-to-ligand charge-transfer (^{3}MLCT) state, which is the level involved in the photoinduced processes. Obviously, the longer-lived the excited state is, the larger the possibility that it is involved in efficient photoinduced processes. This is not only related to bimolecular processes but even to intercomponent acts in photoactive supramolecular arrays.

On the basis of the above cited arguments, it is easy to understand the reason much effort has been recently devoted to the design and synthesis of Ru(II) complexes featuring excited-state lifetimes substantially longer than that of the prototype, $[Ru(bpy)_3]^{2+}$ (bpy = 2,2′-bipyridine). Probably, the most successful approach has been to couple the Ru(II) chromophore with pyrenyl subunits. A seminal work by Ford and Rodgers in the early 1990s[2] indeed demonstrated that an interplay between the metal-based ^{3}MLCT level, and the closely lying pyrene-based triplet state can give rise to mixed chromophores exhibiting prolonged MLCT luminescence, in a manner someway similar to delayed luminescence exhibited by some organic dyes. Following that work, the photophysical properties of several Ru(II) polypyridine complexes containing pyrenyl groups have been reported, notably in the past few years,[3−6] and the study has recently also been extended to other metals.[7,8]

Here, we report a systematic investigation on the absorption spectra and photophysical properties (both at room temperature in fluid acetonitrile solution and at 77 K in rigid matrix) of a large series of Ru(II) and Os(II) complexes containing new polypyridine ligands with appended pyrenyl and/or anthryl chromophores. The number of added organic chromophores per metal complex ranges from 0 to 6, and even mixed pyrenyl/

* To whom correspondence should be addressed. E-mail: photochem@chem.unime.it.
[†] Università di Messina.
[‡] Università di Ferrara. E-mail: idm@dns.unife.it.

10.1021/jp0213497 CCC: $25.00
Published on Web 01/01/2003

TABLE 1: Spectroscopic and Photophysical Data of the Ligands in Degassed Acetonitrile Solution Unless Otherwise Stated

	absorption	luminescence						
		298 K			77 K (fluorescence)[a]		77 K (phosphorescence)[b]	
	λ_{abs}, nm (ϵ, mol^{-1} dm^3 cm^{-1})	λ_{em}[c] nm	τ_{em} ns	ϕ	λ_{em}[c] nm	τ_{em} ns	λ_{em}[c] nm	τ_{em} ms
P	242 (68 650) [^1B_a pyr] 276 (51 480) [^1B_b pyr] 343 (38 400) [^1L_a pyr]	375	190	0.16	375	227	598	0.676
PP	242 (113 203) [^1B_a pyr] 276 (85 901) [^1B_b pyr] 343 (64 640) [^1L_a pyr]	375	210	0.14	375	217	598	0.684
AA	255 (114 752) [^1B_b anth] 390 (8 262) [^1L_a anth]	413	12	0.22	413	12	-	-
AP	276 (43 615) [^1B_b pyr] 343 (37 083) [^1L_a pyr] 390 (8 597) [^1L_a anth]	413	12	0.13	413	13	-	-

[a] Fluorescence data measured at 77 K in butyronitrile rigid matrix. [b] Phosphorescence data measured at 77 K in butyronitrile rigid matrix with addition of ethyl iodide. [c] Highest energy feature of the structured emission band.

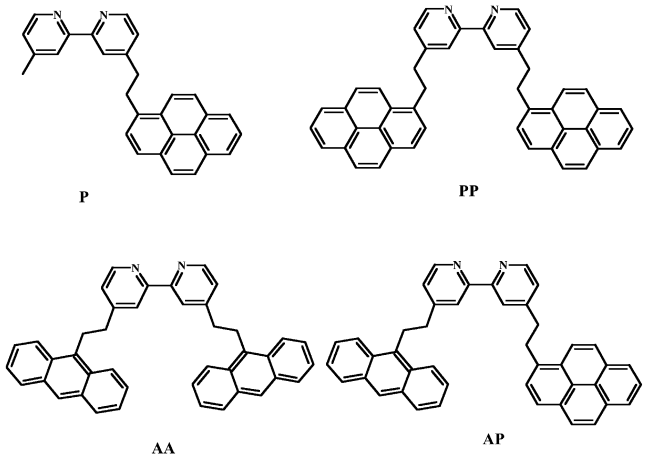

Figure 1. Structural formulas of the pyrenyl- and anthryl-substituted polypyridine ligands.

anthryl-substituted polypyridine ligands are present. To the best of our knowledge, this is also the first case that two different types of chromophores are grafted onto a bipyridine ligand. The absorption and photophysical properties of all of the new free ligands are also reported, along with the synthetic procedures for ligands and complexes. The species studied are the four ligands pyr−bpy (**P**), pyr−bpy−pyr (**PP**), an−bpy−an (**AA**), and an−bpy−pyr (**AP**), whose structural formulas are shown in Figure 1, and the 15 metal complexes $[Ru(dmb)_3]^{2+}$ (**Ru-0**, dmb = 4,4′-dimethyl-2,2′-bipyridine), $[Ru(dmb)_2(P)]^{2+}$ (**Ru-1P**), $[Ru(dmb)_2(PP)]^{2+}$ (**Ru-2Pa**), $[Ru(dmb)(P)_2]^{2+}$ (**Ru-2P**), $[Ru(P)_3]^{2+}$ (**Ru-3P**), $[Ru(dmb)(PP)_2]^{2+}$ (**Ru-4Pa**), $[Ru(P)_2(PP)]^{2+}$ (**Ru-4P**), $[Ru(P)(PP)_2]^{2+}$ (**Ru-5P**), $[Ru(PP)_3]^{2+}$ (**Ru-6P**), $[Ru(AA)_3]^{2+}$ (**Ru-6A**), $[Ru(AP)_3]^{2+}$ (**Ru-3A3P**), $[Os(dmb)_3]^{2+}$ (**Os-0**), $[Os(PP)_3]^{2+}$ (**Os-6P**), $[Os(AA)_3]^{2+}$ (**Os-6A**), and $[Os(AP)_3]^{2+}$ (**Os-3A3P**). All of the metal complexes have been prepared as hexafluorophosphate salts. A schematic representation of the complexes is shown in Figure 2. Preliminary results on some of the Ru(II) complexes has been recently communicated.[6]

Results

The free ligands exhibit intense and structured absorption bands in the UV region (ϵ in the 10^4-10^6 M^{-1} cm^{-1} range), whereas all of the metal complexes exhibit intense structured absorption in the UV region and moderately intense and broad absorption bands in the visible (ϵ in the 10^4-10^5 M^{-1} cm^{-1} range). All of the ligands exhibit a short-lived structured

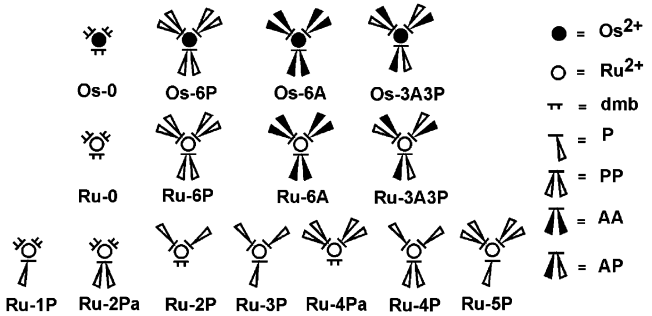

Figure 2. Schematic representation of the metal complexes investigated.

luminescence (lifetime in the nanosecond time scale) both in fluid solution at room temperature and in rigid matrix at 77 K. The species **P** and **PP** also exhibit a long-lived luminescence (millisecond time scale) at 77 K, in the presence of ethyl iodide.

All of the complexes exhibit a single emission, which was fitted by a monoexponential decay, under all of the experimental conditions, except the Ru(II) complexes bearing anthryl substituents, which are luminescent only at 77 K. Among these latter species, **Ru-3A3P** exhibits a double emission at 77 K. The low-temperature emissions are much longer-lived than the corresponding room-temperature emissions. In all cases, the emission spectra are independent of excitation wavelength.

The absorption and photophysical data of the free ligands are collected in Table 1. The absorption spectra and luminescence properties of **AA**, **PP**, and **AP** are shown in Figure 3. The absorption and photophysical properties of all the metal complexes are gathered in Table 2. Figure 4 shows the absorption and luminescence spectra of some representative ruthenium complexes, and Figure 5 shows the absorption and luminescence spectra of the osmium complexes.

The room-temperature transient absorption spectrum measured for **Os-6A** in CH_3CN solution following excitation at 355 nm is shown in Figure 6. The same spectral changes were observed using 532 nm laser excitation. The spectrum is characterized by an absorption maximizing at 425 nm and a bleaching at $\lambda > 450$ nm. In the whole spectral region, the decay of the transient spectral changes follow a good first-order kinetics with a lifetime coincident with that obtained from luminescence experiments (Table 2). The transient spectra of **Os-0** and of the free ligand **AA** are also reported in Figure 6 for comparison. The results of flash photolysis of the complex **Os-3A3P** are qualitatively similar to those obtained for **Os-6A**, with the absorption at 425 nm much weaker.

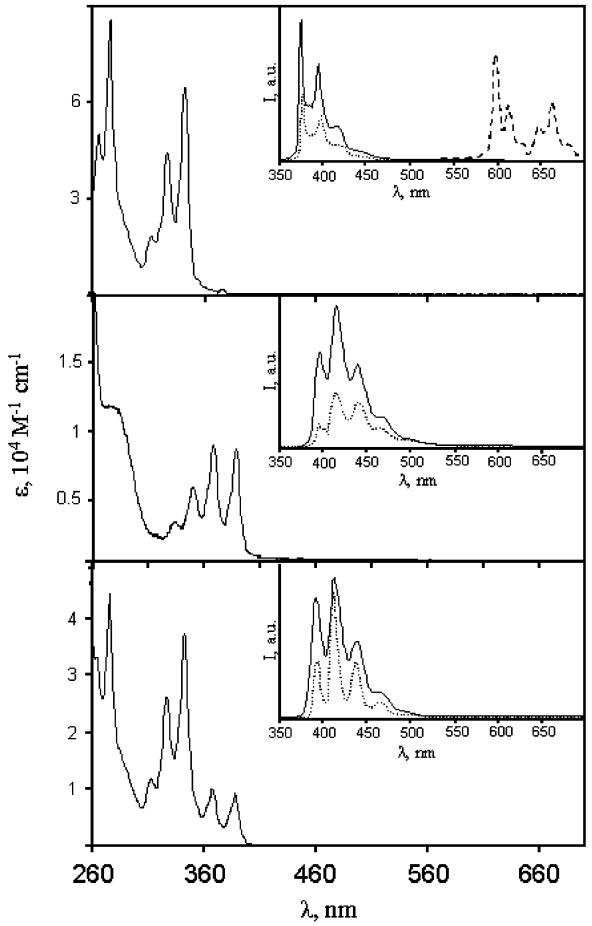

Figure 3. Absorption and (inset) emission spectra of **PP** (top), **AA** (middle), and **AP** (bottom) in acetonitrile solution at room temperature (solid lines) or butyronitrile rigid matrix at 77 K (dotted lines). In the top inset, also the 77 K emission spectrum of **PP** in a butyronitrile/ethyl iodide 9:1 (v/v) matrix is shown (dashed line).

Discussion

Free Ligands. *Absorption Spectra and Room-Temperature Luminescence.* The absorption spectra of the free ligands (Table 1, Figure 3) evidence absorption features typical both of the bipyridine chromophore and of the pyrene and/or the anthracene subunits. The saturated hydrocarbon spacer ensures a relatively high degree of independence of adjacent chromophores. Literature data readily permit the attribution of the various features to specific subunits.[4b,9,10] In particular, the very intense features at 265 and 276 nm which are present in the pyrene-containing species can be attributed to the transitions leading to the population of the ^1B_a and ^1B_b states of the pyrene moieties, respectively; the structured intense bands with maxima at about 345 nm, still present in the pyrene-containing species, can be assigned to the transitions leading to the preparation of the ^1L_a states of the pyrene moieties; the absorption at shorter wavelengths than 260 nm (not shown in Figure) in **AA** and **AP** receives contributions mainly from ^1B_a transitions centered on the anthracene moieties; finally, the structured absorption feature with maxima around 380 nm, which is present in both **AA** and **AP**, is easily recognized as being due to the transitions leading to the preparation of the anthracene-centered ^1L_a states. Bpy-centered $\pi-\pi^*$ absorption bands are expected to appear at about 280 nm, but they are obscured by the more intense anthracene- and pyrene-based bands occurring in the same region.

The absorption spectra seem to be additive, and no particular spectral feature which cannot be assigned to some transitions already occurring in the isolated components is present. This indicates that the mutual interaction (if any) between the various subunits (bipyridine, anthracene, pyrene) of the ligands is weak.

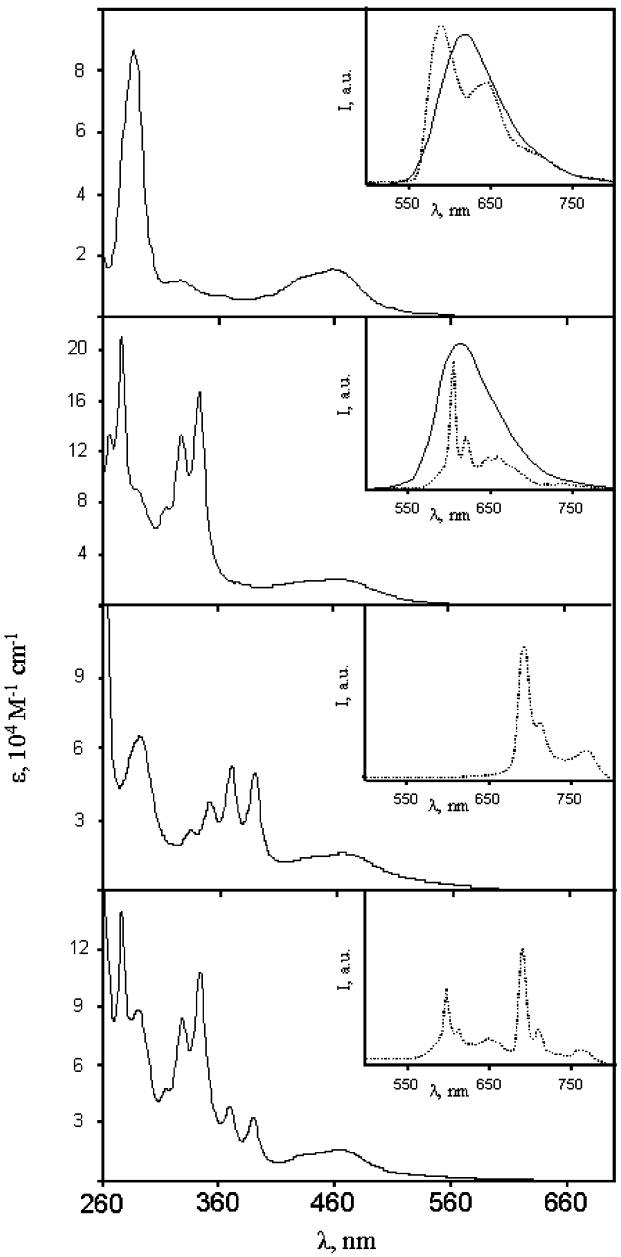

Figure 4. Absorption and (inset) emission spectra of (from the top to the bottom) **Ru-0**, **Ru-6P**, **Ru-6A**, and **Ru-3A3P** in acetonitrile solution at room temperature (solid lines) or butyronitrile rigid matrix at 77 K (dotted lines).

The photophysical properties at room temperature of all of the ligands (Table 1, Figure 3) are dominated by the excited states of the pyrene or anthracene subunits. In acetonitrile solution indeed, the typical structured fluorescence of the pyrene and anthracene chromophores is present. Fluorescence lifetimes and quantum yields are also similar to those of the free pyrene and anthracene,[10] so showing that negligible perturbation of the fluorescent levels of the pyrene and anthracene moieties by the polypyridine fragment takes place. Interestingly, in **PP**, there is no trace of excimer emission, which is indeed quite common in species carrying two pyrene chromophores capable of adopting close contact conformations.[10] Most likely in **PP**, the two pyrenes cannot approach each other in a suitable manner. Moreover, they are probably maintained far from one another

TABLE 2: Spectroscopic and Photophysical Data of the Complexes in Degassed Acetonitrile Solution Unless Otherwise Stated

	absorption	luminescence				
		298K			77K[a]	
	λ_{abs}, nm (ϵ, mol^{-1} dm^3 cm^{-1})	$\lambda_{em\ max}$, nm	τ_{em}	ϕ	$\lambda_{em\ max}$, nm	τ_{em}
Ru-0	286 (86 910) [$\pi-\pi^*$] 457 (15 690) [MLCT Ru]	616	0.87 μs	0.070	595[b]	5 μs
Ru-1P	343 (43 840) [^1L_a pyr] 461 (15 730) [MLCT Ru]	614	2.5 μs	0.065	596[b]	0.733 ms
Ru-2P	343 (82 250) [^1L_a pyr] 459 (14 820) [MLCT Ru]	614	6.6 μs	0.060	597[b]	0.692 ms
Ru-2Pa	343 (85 230) [^1L_a pyr] 463 (15 560) [MLCT Ru]	614	6.9 μs	0.062	597[b]	0.681 ms
Ru-3P	343 (114 900) [^1L_a pyr] 460 (15 130) [MLCT Ru]	614	7.9 μs	0.066	597[b]	0.800 ms
Ru-4P	343 (133 700) [^1L_a pyr] 463 (15 690) [MLCT Ru]	612	11.0 μs	0.053	597[b]	0.774 ms
Ru-4Pa	343 (133 770) [^1L_a pyr] 464 (15 690) [MLCT Ru]	610	11.3 μs	0.054	597[b]	0.650 ms
Ru-5P	343 (156 080) [^1L_a pyr] 464 (15 820) [MLCT Ru]	610	15.0 μs	0.060	598[b]	0.761 ms
Ru-6P	265 (141 380) [^1B_a pyr] 276 (214 650) [^1B_b pyr] 289 (90 030) [$\pi-\pi^*$] 343 (182 280) [^1L_a pyr] 462 (16 770) [MLCT Ru]	608	18.1 μs	0.060	599[b]	0.705 ms
Ru-6A	291 (65 060) [$\pi-\pi^*$] 390 (50 050) [^1L_a anth] 466 (16 020) [MLCT Ru]				691[b]	1.114 ms
Ru-3A3P	276 (139 200) [^1B_b pyr] 290 (88 510) [$\pi-\pi^*$] 344 (108 410) [^1L_a pyr] 390 (32 750) [^1L_a anth] 462 (16 430) [MLCT Ru]				600,[b] 688[b]	0.658 ms 1.396 ms
Os-0	290 (113 050) [$\pi-\pi^*$] 480 (15 360) [MLCT Os] 650 sh (3600) [MLCT Os][c]	745	35.5 ns (29.7 ns)[d]	0.004	728	803 ns
Os-6P	265 (125 090) [^1B_a pyr] 276 (195 880) [^1B_b pyr] 292 (89 300) [$\pi-\pi^*$] 344 (161 440) [^1L_a pyr] 493 (15 320) [MLCT Os] 671 sh (3910) [MLCT Os][c]	731	51.9 ns (40.2 ns)[d]	0.005	717	987 ns
Os-6A	295 (74 200) [$\pi-\pi^*$] 390 (57 075) [^1L_a anth] 493 (15 585) [MLCT Os] 671 sh (4630) [MLCT Os][c]	728	65.3 ns (51.1 ns)[d]	0.006	720	983 ns
Os-3A3P	276 (148 240) [^1B_b pyr] 292 (93 620) [$\pi-\pi^*$] 344 (115 620) [^1L_a pyr] 390 (40 730) [^1L_a anth] 493 (14 600) [MLCT Os] 671 sh (3640)[MLCT Os][c]	732	61 ns (46.2 ns)[d]	0.006	720	979 ns

[a] Data measured at 77 K in butyronitrile rigid matrix. [b] Highest energy feature of the structured emission band. [c] Spin-forbidden MLCT transition. [d] Measured in air-equilibrated acetonitrile solution.

by steric constrains which force the pyridine rings of bpy in a "transoid" conformation, as common for noncoordinated polypyridine fragments.[11] The **AP** free ligand exhibits only the anthracene fluorescence feature regardless of the excitation wavelength used (Figure 3, Table 1): this indicates that efficient singlet−singlet energy transfer from the pyrene subunit to the anthracene one takes place. Definitive support to the energy transfer comes from the excitation spectrum of **AP** (not shown), taken at 450 nm emission wavelength, which displays absorption signatures of both pyrene and anthracene chromophores. Because of the good spectral overlap between pyrene emission and anthracene absorption spectra (Figure 3), the Coulombic mechanism is most likely the mechanism for the energy transfer process.

It should be noted that it has been been reported that in pyrene- and anthracene-substituted polypyridine ligands, CT excited states (pyrene- or anthracene-to-polypyridine) can have a role in determining the photophysical properties of the ligands, and also influence the metal complexes luminescence.[7,8,12,13] However, in all of those cases, the aryl substituents were directly connected to the polypyridine framework. In the systems studied here, the absence of such excited states is attributed to the presence of the alkyl spacers which reduce the CT interaction and are also expected to destabilize the CT excited states.

Luminescence at 77 K. All of the ligands exhibit a single fluorescence emission (Table 1, Figure 3). In all cases, the emission features can be attributed to the fused organic chromophores, almost unperturbed by the polypyridine framework. Even under these conditions, **AP** only shows a single (anthracene-based) fluorescence feature, indicating the occurrence of fast and efficient pyrene-to-anthracene energy transfer also at 77 K. The usual pyrene-based phosphorescence is shown

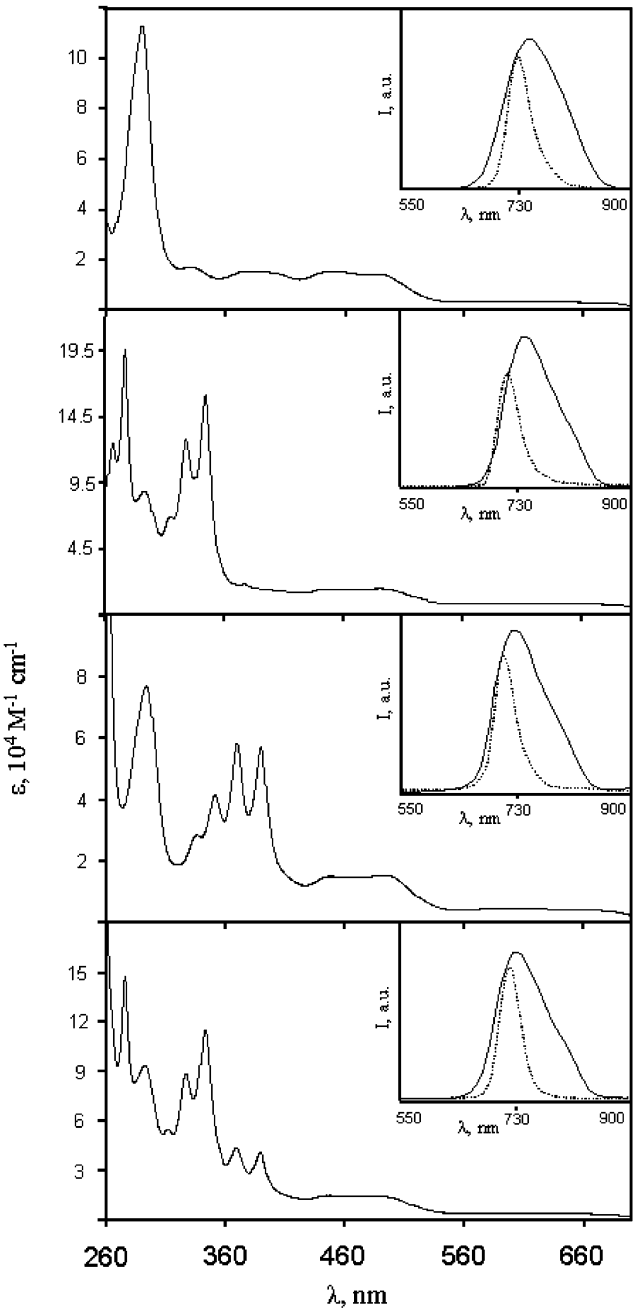

Figure 5. Absorption and (inset) emission spectra of (from the top to the bottom) **Os-0**, **Os-6P**, **Os-6A**, and **Os-3A3P** in acetonitrile solution at room temperature (solid lines) or butyronitrile rigid matrix at 77 K (dotted lines).

in butyronitrile/ethyl iodide 9:1 (v/v) matrix by **P** and **PP**, but **AA** and **AP** do not exhibit any phosphorescence features even in this matrix. Because the anthracene triplet is formed with good yields (as shown by flash photolysis, Figure 6, vide infra), this is probably due to inefficient radiative deactivation of the anthracene triplet to the ground state. Most likely, the pyrene triplet is not populated because of the occurrence of fast singlet−singlet pyrene-to-anthracene energy transfer (see above).

Metal Complexes. The spectroscopic and photophysical properties of transition metal complexes are usually discussed in terms of the localized molecular orbital approximation. Within such an approximation, the electronic transitions and excited states can be described as metal centered (MC), ligand centered (LC), or charge transfer (either metal-to-ligand, MLCT, or ligand-to-metal, LMCT).[9]

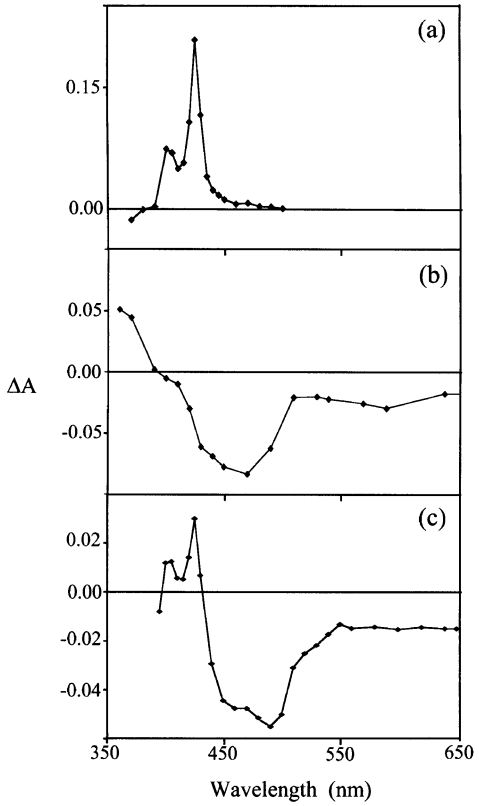

Figure 6. Transient absorption spectra in acetonitrile solution of (a) **AA**, (b) **Os-0**, and (c) **Os-6A**, taken at the end of the laser pulse (half-width 8 ns, $\lambda_{exc} = 355$ nm).

Absorption Spectra. The UV region of all of the complexes is very rich, because of the several possible LC transitions; however, on the basis of the attribution of the various bands made for the free ligands (see above), specific assignment of the absorption features to the various subunits of the multicomponent complexes can be made. Such assignments are straightforward and are reported in detail in Table 2, so they are not discussed further here. A relevant finding to be noted is that the absorption bands are roughly additive (see Table 2). The relatively intense bands in the visible between 400 and 540 nm are assigned to spin-allowed MLCT transitions, whereas the absorption feature at wavelengths longer than 550 nm, exhibited by the Os(II) complexes, are attributed to spin-forbidden MLCT transitions, which gain intensity in the osmium complexes because of enhanced spin−orbit coupling because of the presence of the heavy metal centers.[14] The presence of the anthryl and pyrenyl substituents apparently shifts the absorption MLCT bands of the homoleptic complexes to slightly longer wavelengths (cf. **Ru-0** vs **Ru-6P**, **Ru-6A**, and **Ru-3A3P** and **Os-0** vs **Os-6P**, **Os-6A**, and **Os-3A3P**). This can be attributed to the replacement of the methyl substituents with the aryl-substituted ethyl substituents, which are better σ-electron donor groups than methyls and therefore destabilize the metal-based orbitals, making the metal oxidation, and as a consequence the MLCT transitions, easier.

Photophysical Properties at Room Temperature. On the basis of the luminescence spectra, lifetimes, and quantum yields and a comparison with literature data,[1,9,15] all of the room-temperature emissions exhibited by the metal complexes reported in this work can be attributed to ^{3}MLCT excited states. However, a careful examination of their excited-state lifetimes immediately points out that, in most of the cases, other excited states may also have a role in determining the photophysical properties.

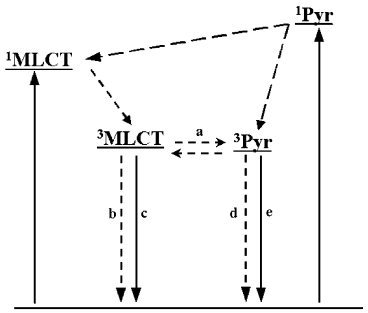

Figure 7. Schematic representation of the energy level diagram and of the possible relaxation processes taking place in the **Ru-nP** series. Solid and dashed lines are radiative and radiationless processes, respectively. Process *a* is an equilibration at room temperature, whereas it is a unidirectional ^{3}MLCT-to-^{3}pyrene energy transfer at 77 K. Processes *b* and *c* are inefficient at 77 K, and processes *d* and *e* are inefficient at room temperature. For details, see text.

As briefly introduced above, ruthenium polypyridine complexes bearing pyrenyl substituents are the subject of a large interest, because of the prolongation of the ^{3}MLCT excited state due to the pyrene-based triplet state.[2−6,8] In these mixed-chromophore species, photoexcitation of the MLCT level is followed by rapid relaxation to an equilibrium mixture of the two triplet states. The same occurs when direct photoexcitation involves the pyrene singlet states (in this case, quantitative quenching of pyrene fluorescence takes place). As previously reported by us in a recent communication,[6] all of the ruthenium complexes containing exclusively additional pyrenyl chromophores investigated here (namely, **Ru-1P**, **Ru-2Pa**, **Ru-2P**, **Ru-3P**, **Ru-4Pa**, **Ru-4P**, **Ru-5P**, and **Ru-6P**) perfectly agree with the adopted equilibrium scheme. Interestingly, it was also stated that the excited-state lifetime of these species is linearly related to the number of appended pyrenyl chromophores but independent of connectivity. Each successive pyrene approximately adds about 2.7 μs to the excited-state lifetime of the complexes in the series (Table 2). In all cases, the decay is strictly monoexponential in the nanosecond time scale, without regard to the excitation wavelength, so the rate constant for the equilibration is assumed to be faster that 1×10^9 s^{-1}. A schematic representation of the decay processes occurring in the Ru-pyrene mixed-chromophore species studied here is shown in Figure 7.

When an equilibration between states takes place, and one of the states does not contribute directy to the luminescence output, as it is the case for the pyrene-based triplet at room temperature, a cost in luminescence quantum yield has to be payed; however, from the data in Table 2, this cost appears to be negligible as the decrease in population of the emitting state is highly balanced by the enhancement in lifetimes.

A somewhat puzzling behavior is represented by the slight blue-shift of the ^{3}MLCT emission band on increasing the number of pyrenyl subunits (compare, for example, **Ru-0** and **Ru-6P** emissions in Table 2), on the basis of the red-shift evidenced by the MLCT absorption band in the same series of complexes (see above). This is tentatively attributed to different perturbations of the singlet and triplet MLCT states by the aryl substituents (or by the replacement of a methyl group with aryl-substituted ethyl groups).

Not surprisingly, **Ru-6A** and **Ru-3A3P** do not exhibit room-temperature emission. It is known that the anthracene triplet lies at lower energy than Ru → bpy CT triplet states, so that the MLCT-to-anthracene triplet energy transfer is not reversible and complete MLCT emission quenching takes places.[4a,15] The schematization of the decay processes in **Ru-3A3P** is shown in Figure 8.

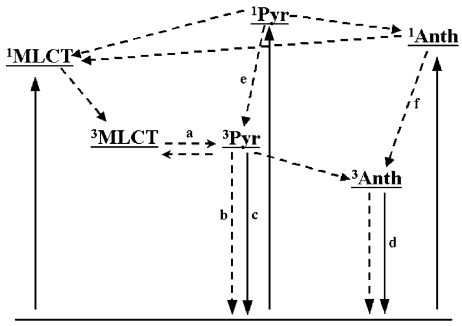

Figure 8. Schematic representation of the energy level diagram and the possible decay processes taking place in **Ru-3A3P**. Solid and dashed lines are radiative and radiationless processes, respectively. Process *a* is an equilibration at room temperature, whereas it is a unidirectional ^{3}MLCT-to-^{3}pyrene energy transfer at 77 K. Processes *b* and *c* are inefficient at room temperature. Process *d* is inefficient at room temperature. Processes *e* and *f* appear to be poorly efficient, at least at 77 K (see main text).

All of the four osmium species **Os-0**, **Os-6P**, **Os-6A**, and **Os-3A3P** exhibit a typical Os-based, ^{3}MLCT emission at room temperature (Table 2, Figure 5). As noted for the ruthenium species, the emission is blue-shifted on passing from **Os-0** to the aryl-substituted complexes, contrary to the shifts in the absorption spectra, suggesting that different perturbation of singlet and triplet states by the aryl substituents also occurs in the osmium complexes. In Os(bpy)$_3$-type species, the emitting ^{3}MLCT level is lower in energy than both pyrene and anthracene triplets, so that neither significant equilibration between excited states or quenching is expected. However, a comparison among the luminescence lifetimes (both in deoxygenated or air-equilibrated solutions, see Table 2) of the four complexes allows us to obtain interesting pieces of information. The luminescence lifetimes of the complexes indeed increase with the number of aryl substituents, namely, the anthryl ones. Partly, the difference in the luminescence lifetimes between **Os-0** and the other species can be attributed to the energy gap law;[16] however, the different values among **Os-6P**, **Os-6A**, and **Os-3A3P** cannot be interpreted in this way, because the energy of the excited state is roughly constant in this series. To explain such an experimental finding, it can be considered that the Os-based ^{3}MLCT state in the aryl-substituted complexes and the anthracene triplet level only differ by about 700 cm^{-1},[17] with the ^{3}MLCT level being the lowest-energy one. This relatively small energy difference allows for population of the higher-energy anthracene triplets at room temperature, according to a Boltzmann distribution.[18] This population would account for the reduced rate constants of the excited-state decays with increasing the number of the anthracene substituents (e.g., the rate constant for radiationless decay k_{nr} passes from 1.92×10^7 s^{-1} for **Os-6P** to 1.63×10^7 s^{-1} for **Os-3A3P** and to 1.53×10^7 s^{-1} for **Os-6A**). Considering the degeneracy of the anthracene triplet levels (in **Os-6A**, there are six isoenergetic anthracene-based triplet states and three in **Os-3A3P**), and assuming that energy transfer rates for forward and back processes between Os-based and anthracene-based triplets greatly exceed intrinsic decays to the ground state, the excited states of **Os-3A3P** and **Os-6A** result to be partitioned between the two levels, with a total 9% or 17% of molecules being in the anthracene-triplet states in the two complexes, respectively. These partitions lead to calculate excited-state lifetimes of 58 and 65 ns for **Os-3A3P** and **Os-6A**, respectively, which are in good agreement with the experimental luminescence lifetime results (Table 2).[19]

The results of flash photolysis experiments strongly confirm the hypothesis given above. The transient spectrum of **Os-6A**

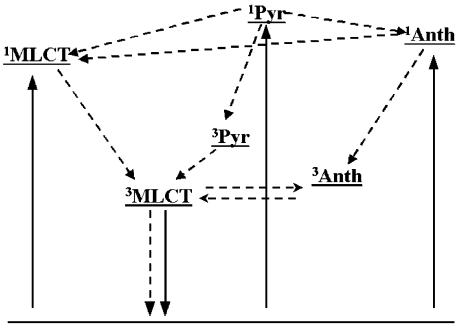

Figure 9. Schematic representation of the energy level diagram and the possible decay processes taking place in **Os-3A3P**. Solid and dashed lines are radiative and radiationless processes, respectively.

(Figure 6) shows the characteristic features of both the triplet of the anthracene subunit (the structured absorption around 410 nm) and of the ^{3}MLCT state (the broad bleaching in the 420−550 nm region), clearly suggesting that, following excitation, a partial population of the anthracene triplet occurs. Both the transient anthracene-based absorption and MLCT bleaching decay with the same rate (lifetime of the transient, 65 (± 2) ns, which is coincident with the luminescence lifetime of **Os-6A**, see Table 2). The transient spectrum of **Os-3A3P** is qualitatively similar to that of **Os-6A**, with the expected difference between the intensity ratio of the anthracene-based absorption and MLCT bleaching (on passing from **Os-6A** to **Os-3A3P**, the intensity of the anthracene absorption is reduced compared to the MLCT bleaching, in agreement with the reduction in the population of the anthracene triplet, see above). Taken together, these findings definitely indicate excited-state equilibration. A schematization of the decay processes occurring in **Os-3A3P** is reported in Figure 9. The effect on luminescence lifetime reported here is small, but in principle, larger effects could be obtained, for example on reducing the energy gap between the relevant excited-state levels.

Finally, for all of the emitting species, excitation spectroscopy indicates that all the features which are present in the absorption spectra of the various complexes contribute quantitatively to the emission. So all of the complexes exhibit an efficient antenna effect, because the light collected by the peripheral, organic chromophores is channelled to a single chromophore. In most of the cases, such a chromophore is the central metal core. All of the aryl-substituted ligands could therefore in principle be part of larger dendrimers as peripheral ligands, giving rise to novel light-harvesting antenna systems. A preliminary investigation in this direction has already been reported as far as the ligand **P** is concerned.[20,21]

Photophysical Properties at 77 K. The ruthenium complex **Ru-0** exhibits emission (Table 2, Figure 4) which can be attributed to ^{3}MLCT excited states, on the basis of emission energy, lifetime, and vibrational progression, which are in agreement with Ru-based ^{3}MLCT luminescence reported in the literature.[9]

The luminescence of **Ru-1P**, **Ru-2Pa**, **Ru-2P**, **Ru-3P**, **Ru-4Pa**, **Ru-4P**, **Ru-5P**, and **Ru-6P** (Table 2, Figure 4) is assigned to pyrene triplet levels. Such an assignment is based on the luminescence lifetimes (e.g., cf. the data in Table 2 with the lifetime of an alkylpyrene[2]), and on the emission profiles, which are slightly different from that of **Ru-0** and similar to that of the free pyrenyl-substituted ligands, see Figure 3). In principle, for all of these multichromophoric species, one could expect two emission features, namely, the pyrene triplet and the MLCT level lying at almost the same energy. However, even exciting directly into the intense ^{1}MLCT absorption bands, only the monoexponential decaying, pyrene-based phosphorescence is found in all of the complexes, with no traces of any component decaying with a faster rate (at least in the ns time regime). This indicates that no equilibration takes place at 77 K, as expected, and that fast energy transfer from the MLCT excited state to the pyrene triplet state(s) takes place. The luminescence of **Ru-6A** (Table 2, Figure 4) is attributed to the anthracene triplet state, on the basis of emission energy, profile, and lifetime, and according to literature data concerning the luminescence properties of mononuclear Ru(II) complexes containing anthracene subunits.[4,22]

Interestingly, **Ru-3A3P** displays emission features which can be attributed to both anthracene- and pyrene-based phosphorescence (Table 2, Figure 4). Also the emission spectrum for this complex is not dependent on excitation wavelength. This demonstrates that direct population of the pyrene and anthracene singlet absorption bands leads in each case to population of the ^{3}MLCT state (probably via the ^{1}MLCT level), and the electronic energy is then redistributed to the lower-lying pyrene and anthracene triplets by energy transfer processes. This also implies that the pyrene and anthracene singlet states do not directly decay to their respective triplet states in a significant way (see Figure 8). In fact, if direct pyrene- or anthracene-centered singlets should substantially lead directly to their triplet (emitting) levels, the 77 K emission spectrum of **Ru-3A3P** would be excitation-wavelength-dependent, in contrast to the experimental results.

It can be noted that the lifetime of the higher-energy emission feature (the pyrene-based emission) in **Ru-3A3P** is almost identical to that of the emission of **Ru-6P**. This indicates that energy transfer from the pyrene triplet level to the anthracene triplet state is inefficient under these experimental conditions. It should be recalled that energy transfer from the singlet ^1L_a pyrene state to the singlet ^1L_a anthracene state, occurring with a high efficiency in the free ligand **AP** as demonstrated by the luminescence of this latter species at room temperature, can occur via a Coulombic mechanism, taking advantage of the good overlap between donor emission and acceptor absorption spectra (see above). This mechanism cannot be efficient for energy transfer between the corresponding triplet states. At room temperature, triplet−triplet pyrene-to-anthracene energy transfer in metal complexes (which can be an efficient process, as inferred by the room-temperature luminescence properties of **Ru-3A3P**, where probably an electron exchange mechanism is operating) can be mediated by the ^{3}MLCT state, but this latter state can hardly be involved in the energy transfer process at 77 K.

Luminescence of all of the four osmium complexes is attributed to the Os-based ^{3}MLCT excited state, which is the lowest-energy level in all of the species. As seen for the room-temperature emission, luminescence of **Os-0** occurs at lower energy than those of the other osmium species (Table 2, Figure 5). Luminescence lifetimes of the species containing the aryl-substituted ligands (i.e., **Os-6A**, **Os-6P**, and **Os-3A3P**) are longer-lived compared to that of **Os-0**, in accordance with the energy gap law. However, unlike the room temperature lifetimes, they are identical to one another. As we interpreted the differences in room-temperature emission lifetimes among these three complexes on the basis of a Boltzmann distribution, the 77 K results are easily interpreted by considering that the higher-energy anthracene-based levels are no longer accessible at low temperature.

Experimental Section

Equipment and Procedures. The solvents used were of the best spectroscopic grade and were used without further purification. NMR spectra were recorded on a Bruker AC 250 spectrometer (250 MHz). Absorption spectra were recorded with a Kontron Uvikon 860 spectrophotometer. Luminescence spectra were recorded on a Jobin-Yvon Spex Fluoromax-2 spectrofluorimeter, equipped with a red-sensitive Hamamatsu R3896 photomultiplier. Luminescence spectra are uncorrected for detector response. For the luminescence lifetimes in the nanosecond to microsecond ranges, an Edinburgh OB900 time-correlated single-photon-counting spetrometer has been employed (sources: (i) Hamamatsu PLP 2 laser diode, output, 408 nm, pulse width, 57 ps, or (ii) nitrogen discharge, pulse width, 2 ns), whereas for the luminescence lifetimes in the millisecond time range, a Perkin-Elmer LS-5B spectrofluorimeter was used, with variable delay times and fixed gate times (2 ms). In all cases, the decays were strictly monoexponential. The latter spectrofluorimeter was also used to record the phosphorescence spectra of the free ligands, by using a delay time of 1 μs to eliminate contributions from fluorescence. Luminescence quantum yields have been calculated by using the optically diluted method.[23] As quantum yield references, we used $[Ru(bpy)_3]^{2+}$ in aerated aqueous solution ($\Phi = 0.028$[24]) for the ruthenium complexes, $[Os(bpy)_3]^{2+}$ in deaerated acetonitrile solution ($\Phi = 0.005$[25]) for the osmium species, and anthracene in deaerated ethanol solution ($\Phi = 0.27$[26]) for the free ligands. Nanosecond flash photolysis transient absorption experiments were performed with a Continuum Surelight Nd:YAG laser as excitation source by using an apparatus previously described.[27] All measurements were carried out on deaerated solutions.

The experimental uncertainties are as follows: absorption and luminescence maxima, 2 nm; luminescence lifetimes, 5%, transient decay rates, 5%, luminescence quantum yields, 20%.

Synthesis. *General Notes.* All manipulations were performed under a dry nitrogen atmosphere using standard techniques, while protecting against light. 4,4′-Dimethyl-2,2′-bipyridine (dmb), lithium diisopropylamide (2 Molar), 1-pyrenemethanol, ruthenium(III)chloride hydrate, and potassium hexachloroosmate (IV) were obtained from Aldrich and used as received. THF (Aldrich) was distilled immediately before use. Neutral alumina (Aldrich) was used in column chromatography. 1-(Chloromethyl)pyrene,[28] 9-(bromomethyl)anthracene,[29] $[Ru(dmb)_3](PF_6)_2$[30] (**Ru-0**), and $[Os(dmb)_3](PF_6)_2$[31] (**Os-0**) were prepared according to published procedures. The synthesis of the ligands **P** and **PP** as well as of the complexes **Ru-nP** has been reported elsewhere.[6,20]

Synthesis of Ligands an−bpy−an (AA) and an−bpy−pyr (AP). 4,4′-Bis[2-(9-anthryl)ethyl]-2,2′-bipyridine (AA). 4,4′-Dimethyl-2,2′-bipyridine (0.50 g, 2.71 mmol) was dissolved in dry THF (40 mL) under a nitrogen atmosphere. After cooling to −10 °C, lithium diisopropylamide (3.0 mL) was added dropwise over a 5 min period via syringe. After stirring for an additional 45 min, a solution of 9-(bromomethyl)anthracene (1.63 g, 6.00 mmol) in THF (40 mL) was introduced dropwise by cannula. The reaction mixture was stirred at −10 °C for 45 min, and then allowed to warm to ambient temperature and reacted for a further 20 h. After this time, water (5 mL) was added dropwise, and solvents were removed under reduced pressure. The residue was then dissolved in dichloromethane and washed with water. The separated organic phase was dried over magnesium sulfate and filtered, and the solvent was removed. The residue was then triturated with methanol:water, 4:1 v/v (20 mL). The resulting solid was collected and then triturated twice with methanol (2 × 25 mL) and repeatedly with diethyl ether (4 × 40 mL). The product, which was collected by filtration and dried under vacuum, was an off-white powder (yield: 68%). ^{1}H NMR ($CDCl_3$): δ 8.68 (d, 2H, $J = 5$ Hz), 8.53 (s, 2H), 8.41 (s, 2H), 8.33 (d, 4H, $J = 9$ Hz), 8.04 (d, 4H, $J = 9$ Hz), 7.48−7.58 (m, 8H), 7.31 (d, 2H, $J = 5$ Hz), 4.02 (t, 2H, $J = 8$ Hz), 3.22 (t, 2H, $J = 8$ Hz). Elemental analysis data (for $C_{42}H_{32}N_2$), calc. (found): C, 89.40 (89.33); H, 5.59 (5.71); N, 4.91% (4.96%). MS (FAB): *m*/*z* 564.

4-[2-(9-Anthryl)ethyl]-4′-[2-(1-pyrenyl)ethyl]-2,2′-dipyridine (AP). 4-[2-(9-Anthryl)ethyl]-4′-methyl-2,2′-bipyridine[32] (0.55 g, 1.47 mmol) was dissolved in dry THF (40 mL) under a nitrogen atmosphere. After cooling to −10 °C, lithium diisopropylamide (0.9 mL) was added dropwise over a 5 min period via syringe. After stirring for an additional 45 min, a solution of 1-(chloromethyl)pyrene (0.37 g, 1.47 mmol) in THF (25 mL) was introduced dropwise by cannula. Employing similar reaction conditions and workup procedure as described for **AA** gave a pale yellow powder (yield: 54%). ^{1}H NMR ($CDCl_3$): δ 8.70−8.61 (m, 2H), 8.50 (s, 1H), 8.45 (s, 1H), 8.42 (s, 1H), 8.39−8.29 (m, 3H), 8.25−7.97 (m, 9H), 7.87 (dd, 1H), 7.63−7.46 (m, 4H), 7.31 (dd, 1H), 7.17 (dd, 1H), 4.01 (t, 2H, $J = 8$ Hz), 3.77 (t, 2H, $J = 8$ Hz), 3.36−3.15 (m, 4H). Elemental analysis data (for $C_{44}H_{32}N_2$), calc. (found): C, 90.16 (89.76); H, 5.34 (5.48); N, 4.57 (4.76). MS (FAB): *m*/*z* 588.

Synthesis of Metal Complexes. $[Ru(AA)_3](PF_6)_2$ (Ru-6A), $[Os(AA)_3](PF_6)_2$ (Os-6A), $[Os(PP)_3](PF_6)_2$ (Os-6P), $[Ru(AP)_3](PF_6)_2$ (Ru-3A3P), $[Os(AP)_3](PF_6)_2$ (Os-3A3P). In a typical synthesis, $RuCl_3 \cdot 3H_2O$ (or K_2OsCl_6) (0.15 mmol) and ligand L (L = **AA**, **PP** or **AP**) (0.45 mmol) were dissolved in DMF (6 mL) and refluxed for 24 h under nitrogen. After cooling to room temperature, excess solid NH_4PF_6 was added. The solution was left to stir for 30 min, before loading onto a column of neutral alumina, and eluting with acetonitrile:toluene, 2:1 v/v. Solvent was removed under reduced pressure until a precipitate was obtained. The solid was collected by vacuum filtration through a fine glass frit and washed with water, followed by diethyl ether. The complex was further purified through Sephadex G10, eluting with acetonitrile, before reprecipitating from acetonitrile/toluene. Elemental analysis and mass data were in agreement with the proposed structures.

Acknowledgment. We thank Prof. Franco Scandola for helpful discussions. CNR-Agenzia 2000, Università di Messina, and EC-TMR Network on Nanometer Size Metal Complexes are acknowledged for financial support.

Supporting Information Available: Kinetic profiles of the transient decays of **Os-0** and **Os-6A**, recorded at 480 nm. This material is available free of charge via the Internet at http://pubs.acs.org.

References and Notes

(1) (a) Balzani, V.; Scandola, F. *Supramolecular Photochemistry*; Horwood: Chichester, 1991. (b) Sauvage, J.-P.; Collin, J. P.; Chambron, J.-C.; Guillerez, S.; Coudret, C.; Balzani, V.; Barigelletti, F.; De Cola, L.; Flamigni, L. *Chem. Rev.* **1994**, *94*, 993. (c) Balzani, V.; Juris, A.; Venturi, M.; Campagna, S.; Serroni, S. *Chem. Rev.* **1996**, *96*, 956 and references therein. (d) Harriman, A.; Ziessel, R. *Chem. Commun.* **1996**, 1707. (e) Bignozzi, C. A.; Schoonover, J. R.; Scandola, F. *Progr. Inorg. Chem.* **1997**, *44*, 1. (f) De Cola, L.; Belser, P. *Coord. Chem. Rev.* **1998**, *177*, 301. (g) Barigelletti, F.; Flamigni, L. *Chem. Soc. Rev.* **2000**, *29*, 1. (h) Sun, L.; Hammarstroem, L.; Akermark, B.; Styring, S. *Chem. Soc. Rev.* **2001**, *30*, 36. (i) Ballardini, R.; Balzani, V.; Credi, A.; Gandolfi, M. T.; Venturi, M. *Acc. Chem. Res.* **2001**, *34*, 445. (l) Pomeranc, D.; Heitz, V.; Chambron, J.-C.; Sauvage, J.-P. *J. Am. Chem. Soc.* **2001**, *123*, 12215. (m) Fleming, C.

N.; Maxwell, K. A.; De Simone, J. M.; Meyer, T. J.; Papanikolas, J. M. *J. Am. Chem. Soc.* **2001**, *123*, 10336.

(2) Ford, W. E.; Rodgers, M. A. J. *J. Phys. Chem.* **1992**, *96*, 2917.

(3) (a) Tyson, D. S.; Castellano, F. N. *J. Phys. Chem. A* **1999**, *103*, 10955. (b) Tyson, D. S.; Henbest, K. B.; Bialecki, J.; Castellano, F. N. *J. Phys. Chem. A* **2001**, *105*, 8154. (c) Tyson, D. S.; Luman, C. R.; Zhou, X.; Castellano, F. N. *Inorg. Chem.* **2001**, *40*, 4063.

(4) (a) Wilson, G. J.; Sasse, W. H. F.; Mau, A. W.-H. *Chem. Phys. Lett.* **1996**, *250*, 583. (b) Wilson, G. J.; Launikonis, A.; Sasse, W. H. F.; Mau, A. W.-H. *J. Phys. Chem. A* **1997**, *101*, 4860.

(5) (a) Simon, J. A.; Curry, S. L.; Schmehl, R. H.; Schatz, T. R.; Piotrowiak, P.; Jin, X.; Thummel, R. P. *J. Am. Chem. Soc.* **1997**, *119*, 11012. (b) Hissler, M.; Harriman, A.; Khatyr, A.; Ziessel, R. *Chem. Eur. J.* **1999**, *5*, 3366. (c) Thorton, N.; Schanze, K. S. *New J. Chem.* **1996**, *20*, 791. (d) Juris, A.; Prodi, L. *New J. Chem.* **2001**, *25*, 1132.

(6) McClenaghan, N. D.; Barigelletti, F.; Maubert, B.; Campagna, S. *Chem. Commun.* **2002**, 602.

(7) Michalec, J. F.; Bejune, S. A.; Cuttell, D. G.; Summerton, G. C.; Gertenbach, J. A.; Field, J. S.; Haines, R. J.; McMillin, D. R. *Inorg. Chem.* **2001**, *40*, 2193.

(8) Del Guerzo, A.; Leroy, S.; Fages, F.; Schmehl, R. H. *Inorg. Chem.* **2002**, *41*, 359.

(9) Juris, A.; Balzani, V.; Barigelletti, F.; Campagna, S.; Belser, P.; von Zelewsky, A. *Coord. Chem. Rev.* **1988**, *84*, 85.

(10) Klessinger, M.; Michl, J. *Excited States and Photochemistry of Organic Molecules*; Wiley: New York, 1995.

(11) Lehn, J.-M. *Supramolecular Chemistry*; VCH−Wiley: Weinheim, Germany, 1995.

(12) Credi, A.; Balzani, V.; Campagna, S.; Hanan, G. S.; Arana, C. R.; Lehn, J.-M. *Chem. Phys. Lett.* **1995**, *243*, 105.

(13) Albano, G.; Balzani, V.; Constable, E. C.; Maestri, M.; Smith, D. R. *Inorg. Chim. Acta* **1998**, *277*, 225.

(14) (a) Kober, E. M.; Caspar, J. V.; Sullivan, B. P.; Meyer, T. J. *Inorg. Chem.* **1988**, *27*, 4587. (b) Denti, G.; Serroni, S.; Sabatino, L.; Ciano, M.; Ricevuto, V.; Campagna, S. *Gazz. Chim. Ital.* **1991**, *121*, 37.

(15) (a) Boyde, S.; Strouse, G. F.; Jones, W. E., Jr.; Meyer, T. J. *J. Am. Chem. Soc.* **1989**, *111*, 7448. (b) Younathan, J. N.; Jones, W. E.; Meyer, T. J. *J. Phys. Chem.* **1991**, *95*, 488. (c) Belser, P.; Dux, R.; Baak, M.; De Cola, L.; Balzani, V. *Angew. Chem., Intern. Ed. Engl.* **1995**, *34*, 595.

(16) (a) Siebrand, W. *J. Chem. Phys.* **1967**, *46*, 440. (b) Caspar, J. V.; Meyer, T. J. *J. Phys. Chem.* **1983**, *87*, 952.

(17) The ^{3}MLCT-triplet anthracene energy gap has been evaluated by assuming the 77 K emission maxima of **Os-6A** and of **Ru-6A** (Table 2) as the energy levels of the two states, respectively.

(18) A similar result has been obtained for another mixed anthracene−Os(II) complex (El-ghayoury, A.; Harriman, A.; Ziessel, R. *Chem. Commun.* **1999**, 2027). Alternatively, it could be suggested that partial mixing between MLCT and anthracene triplets could occur. However, this seems to be less probable considering that the ethyl bridges only allow for small couplings.

(19) The Boltzmann distribution is espressed by the general formula: $n_j/N = [g_i e^{-E_i/k_B T}]/q$, where g_i is the degeneracy of the i level, E_i is the energy difference between the states, k_B is the Boltzmann constant, and q is the molecular partition function, taken as: $q = \sum_i g_i e^{-E_i/k_B T}$. Assuming $E_i = 700$ cm^{-1}, and considering the degeneracy of the upper-lying anthracene triplets, the values reported in the main text for the population of the anthracene-triplet states in **Os-6A** and **Os-3A3P** are obtained (only the first two terms in the summation expressing the molecular partition function are considered). The overall lifetime of the equilibrated excited state is obtained by assuming as the deactivation rate constant for the ^{3}MLCT state that obtained from the room-temperature emission lifetime of **Os-6P** (52 ns) and for the anthracene triplet the deactivation rate constant obtained from the lifetime of the transient absorption in a Ru(II) complex reported in ref 4b (350 μs).

(20) McClenaghan, N. D.; Loiseau, F.; Puntoriero, F.; Serroni, S.; Campagna, S. *Chem. Commun.* **2001**, 2634.

(21) For recent reviews on metal-based dendrimers as artificial light-harvesting antennas, see: Balzani, V.; Ceroni, P.; Juris, A.; Venturi, M.; Campagna, S.; Puntoriero, F.; Serroni, S. *Coord. Chem. Rev.* **2001**, *219*−*221*, 545.

(22) Serroni, S.; Campagna, S.; Pistone Nascone, R.; Hanan, G. S.; Davidson, G. J.; Lehn, J.-M. *Chem. Eur. J.* **1999**, *5*, 3523.

(23) Demas, J. N.; Crosby, G. A. *J. Phys. Chem.* **1971**, *75*, 991.

(24) Nakamaru, N. *Bull. Chem. Soc. Jpn.* **1982**, *55*, 2697.

(25) Kober, E. M.; Caspar, J. V.; Lumpkin, R. S.; Meyer, T. J. *J. Phys. Chem.* **1986**, *90*, 3722.

(26) Dawson, W. R.; Windsor, M. W. *J. Phys. Chem.* **1968**, *72*, 3251.

(27) Kleverlaan, C. J.; Indelli, M. T.; Bignozzi, C. A.; Pavanin, L.; Scandola, F.; Hasselman, G. M.; Meyer, T. J. *J. Am. Chem. Soc.* **2002**, *122*, 2840.

(28) Bair, K. W.; Tuttle, R. L.; Knick, V. C.; Cory, M.; McKee, D. D. *J. Med. Chem.* **1990**, *33*, 2385.

(29) Bullpit, M.; Kitching, W. *J. Org. Chem.* **1976**, *41*, 760.

(30) Damrauer, N. H.; Boussie, T. R.; Devenney, M.; McCusker, J. K. *J. Am. Chem. Soc.* **1997**, *119*, 8253.

(31) Johnson, S. A.; Westmoreland, T. D.; Caspar, J. V.; Barqawi, K. R.; Meyer, T. J. *Inorg. Chem.* **1988**, *27*, 3195.

(32) Weinheimer, C.; Choi, Y.; Caldwell, T.; Gresham, P.; Olmsted, J., III. *J. Photochem. Photobiol. A: Chem.* **1994**, *78*, 119.